Complete phase and amplitude synchronization of broadband chaotic optical fields generated by semiconductor lasers subject to optical injection

How-foo Chen and Jia-ming Liu
Department of Electrical Engineering, University of California, Los Angeles, Los Angeles, California 90095-159410, USA
(Received 9 April 2003; revised manuscript received 11 August 2004; published 29 April 2005)

A direct experimental observation of phase synchronization, amplitude synchronization, and frequency locking for the high-frequency broadband chaotic optical fields of the transmitter and the receiver is demonstrated in a fully optical system, where its chaotic optical wave form is generated through the high-speed nonlinearity of semiconductor lasers subject to optical injection. This experimentally achieved chaotic synchronous scenario is verified as identical chaos synchronization by observing several key characteristics of chaos synchronization in this system. The observation at the frequency detuning, the phase sensitivity, and the effect of mismatch at the injection strength from the master laser and match at the laser output power is in good agreement with the theoretical analysis of this system.

DOI: 10.1103/PhysRevE.71.046216 PACS number(s): 05.45.Xt, 05.45.Vx

I. INTRODUCTION

Synchronization of nonlinear oscillators is a general phenomenon occurring in nature. Among several different synchronization scenarios, the studies and investigations of chaos synchronization have aroused great attention due to its potential applications in security communications [1,2]. Besides the development in communications, progress in this field has extended to biology, chemistry, and control engineering underlying different synchronization criteria of chaotic systems [3–6].

Optical chaos synchronization utilizing semiconductor lasers has attracted much attention for its potential applications in high-speed private communications [7,8]. Due to their rich and fast nonlinear dynamics, as well as the advantage of relatively easy manipulation, semiconductor lasers are considered good candidates for investigating the general characteristics of coupled nonlinear oscillators with different chaotic states, especially for the synchronization of nonlinear oscillators with subnanosecond dynamics. The nonlinear dynamics of semiconductor lasers can be classified based on the different perturbations applied to them. Three main systems—namely, optical injection, optical feedback, and optoelectronic feedback systems— have been considered as the main semiconductor laser systems for the study of nonlinear dynamics. Because of their rich dynamics and related applications especially in optical communications, their dynamics have been extensively studied through numerical simulations, numerical analysis, and experiments [9–12].

Although chaos synchronization utilizing the nonlinearity of semiconductor lasers has been extensively studied in theory and in experiment [8,13–17], the experiments have been focused on delay systems, such as optical feedback systems and optoelectronic feedback systems. It has been pointed out that the chaos synchronization of delay feedback systems has the characteristics of retarded synchronization and anticipated synchronization by Voss [18]. The characteristics have been further studied by Ciszak *et al.* [6] and Heil *et al.* [19]. These general characteristics of delay feedback systems have been proposed to used in control systems [6] based on the fact that the receiver can predict the unstable behavior of the transmitter. In these systems, the quasiperiodic route to chaos is the main characteristic of the nonlinear dynamics and the main mechanism to drive the systems into chaotic states. The delay systems usually have a strong frequency component corresponding to the inverse of the feedback delay time. Therefore, the wave forms usually show strong correlation in quasiperiod corresponding to the feedback delay time [20]. Different from the delay systems, we report an experimental study of a coupled semiconductor laser system subject to an external monochromatic optical field: namely, the optical injection system. While the delay systems represent nonlinear oscillators with self-control or self-perturbation mechanisms, the injection system represents nonlinear oscillators with an external harmonic control or perturbation mechanism. From numerical simulations, numerical analysis, and experiments, a rich nonlinear dynamics of optical injected semiconductor lasers has been reported, and several routes to chaos—namely, period-doubling bifurcation, quasiperiodic bifurcation, and a mixture of both [21]—have been numerically analyzed based on a bifurcation analysis [22]. The periodlike correlation on the wave form observed in delay systems does not appear in the optical injection system [20].

In general, for a fully optical system such as the optical injection system [14], in which the entire optical field is involved in the chaotic dynamics of the lasers, true identical chaos synchronization requires the simultaneous synchronization of the slow-varying phase, the fast-varying optical phase, and the intensity of the chaotic wave form, as well as a locking of the optical frequency between the transmitter and receiver lasers. In this paper, we report a direct experimental observation of chaotic phase synchronization in a fully optical semiconductor laser system, which performs identical chaos synchronization. The chaotic wave form is generated by the high-speed nonlinearity of semiconductor lasers subject to optical injection [9]. The synchronization of the slow-varying phase in a gigahertz range, as well as that of the fast-varying optical phase at the optical frequency, is verified through optical interference when the intensity is

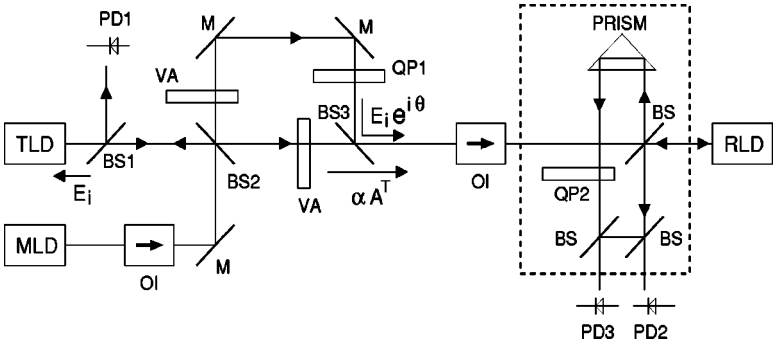

FIG. 1. Schematic setup of the experiment. E_i is the injection field from the master laser. MLD: master laser diode. TLD: transmitter laser diode. RLD: receiver laser diode. PD: photodetector-amplifier combination. BS: beam splitter. VA: variable attenuator. M: mirror. QP: quartz plate. OI: optical isolator.

synchronized. It is found that frequency locking has to be accomplished first for phase synchronization in this system to be possible. Together with the synchronization of intensity, the entire optical output fields of two lasers are completely synchronized once such frequency locking and phase synchronization are accomplished. As is predicted by a theoretical analysis [14], the achieved synchronization can be completely destroyed when the relative optical phase between the transmitter laser output and the master laser (MLD) output is not properly adjusted. The observed frequency detuning between the free-running frequencies of the transmitter and receiver also agrees with what the chaos synchronization theory of this system anticipated. The output powers of both transmitter and receiver lasers are the same when synchronization is achieved. Since the transmitter and receiver are both subject to optical injection from the master laser in order to keep the configurations of both lasers identical, the effect of the optical injection mismatch on the synchronization is also investigated by the removal of the optical injection to the receiver.

II. EXPERIMENTAL SETUP

The schematic setup of the experiment is shown in Fig. 1. The output of the MLD is split into two beams through the beam splitter BS2: The one denoted by $E_i(t)$ is injected into the transmitter to drive the transmitter into chaotic states, and the other beam denoted by $E_i(t)e^{i\theta}$ is injected into the receiver together with the output of the transmitter at BS3. The existence of the relative optical phase θ can be realized from the fact that the optical field of the transmitter encounters the output field of the MLD twice. The first time occurs inside the transmitter laser and the second time at BS3. The phase θ defines the optical phase difference between these two encounters for the same optical field of the transmitter [14]. The phase θ is controlled by tilting QP1 in a small angle. Synchronization on the slow-varying phase, as well as that on the fast-varying optical phase, is detected through the interferometer highlighted by the dashed box. When synchronization of both phases is achieved simultaneously, constructive interference or destructive interference can be detected by the detector PD3 by adjusting the relative optical phase between the transmitter output and the receiver output when they interfere with each other. This relative optical phase is adjusted by the quartz plate QP2. The detectors PD1 and PD2 are used to detect the transmitter output and the receiver output, respectively. Two two-stage optical isolators (OI) with 60-dB isolation are used in the experiment.

The semiconductor lasers used in this setup are InGaAsP/InP single-mode distributed feedback (DFB) semiconductor lasers obtained from Rockwell as laboratory products. The emitting wavelength is around 1.295 μm. The lasers are all fabricated from the same wafer and selected by the close match of their intrinsic laser parameters that are found through experimental measurements [25]. The photodetectors used to detect the outputs of the transmitter and the receiver are InGaAs photodetectors with a 3-dB bandwidth of 6 GHz. The electrical signal from the output of each detector is amplified by an HP 83006A microwave amplifier with a bandwidth covering the range from 0.01 GHz to 26.5 GHz and a gain of 23 dB. The output of the transmitter laser and that of the receiver laser after amplification are recorded in the time domain by a Tektronix TDS 694C digitizing sampling oscilloscope that has a 3 -GHz bandwidth and a sampling rate of 10 GS/s for four channels simultaneously. The power spectra of the laser outputs are taken with an HP E4407B spectrum analyzer with a bandwidth ranging from 9 kHz to 26.5 GHz. The optical frequency of each laser is measured by an Advantest Q8347 optical spectrum analyzer with a resolution of 0.005 nm.

III. THEORETICAL CONSIDERATION

In the experiment, the chaotic wave form is generated by injecting $E_i(t)$ to the transmitter laser, which can be dynamically modeled with the following coupled equations [23]:

$$\frac{dA^T}{dt} = -\frac{\gamma_c^T}{2}A^T + i(\omega_0^T - \omega_c^T)A^T + \frac{\Gamma}{2}(1 - ib^T)g^T A^T + F_{sp}^T + \eta E_i(t),$$

$$\frac{dN^T}{dt} = \frac{J^T}{ed} - \gamma_s^T N^T - \frac{2\epsilon_0 n^2}{\hbar\omega_0^T} g^T |A^T|^2.$$

Meanwhile, the dynamics of the receiver, injected by the channel signal consisting of the transmitter output αA^T and the optical field $E_i(t)e^{i\theta}$ from the MLD, is modeled with the following equations [14]:

$$\frac{dA^R}{dt} = -\frac{\gamma_c^R - 2\alpha\eta}{2}A^R + i(\omega_0^T - \omega_c^T + \Delta\omega_c)A^R + \frac{\Gamma}{2}(1 - ib^R)g^R A^R + F_{sp}^R + \eta E_i(t)e^{i\theta} + \alpha\eta(A^T - A^R),$$

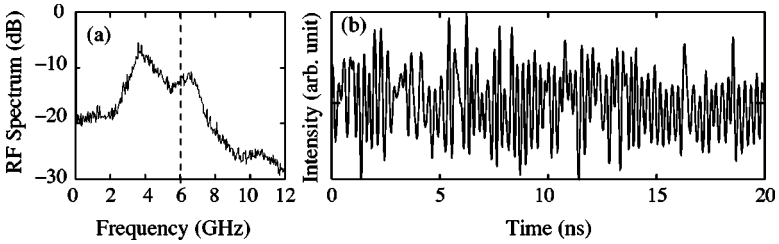

FIG. 2. Experimental measurement of chaotic output of the transmitter: (a) is the power spectrum; (b) is the intensity wave form. Dashed line in (a) indicates the 3-dB bandwidth, 6 GHz, of the photodiode used for obtaining the power spectrum. In reality, the power spectrum beyond 6 GHz is higher than the data shown here.

$$\frac{dN^{\mathrm{R}}}{dt} = \frac{J^{\mathrm{R}}}{ed} - \gamma_{\mathrm{s}}^{\mathrm{R}} N^{\mathrm{R}} - \frac{2\epsilon_0 n^2}{\hbar \omega_0^{\mathrm{T}}} g^{\mathrm{R}} |A^{\mathrm{R}}|^2,$$

where the superscripts T and R indicate the transmitter and receiver, respectively, A is the total complex intracavity field amplitude at the free-running frequency, $\omega_0^{\mathrm{T}}/2\pi$, of the transmitter, γ_{c} is the cavity decay rate, ω_{c} is the longitudinal mode frequency of the cold laser cavity, $\Delta\omega_{\mathrm{c}} = \omega_{\mathrm{c}}^{\mathrm{T}} - \omega_{\mathrm{c}}^{\mathrm{R}}$ is the difference between the cold-cavity frequencies of the transmitter and receiver, Γ is the confinement factor, b is the linewidth enhancement factor, g is the optical gain coefficient including nonlinear effects, F_{sp} is the spontaneous emission noise source, η is the injection coupling rate, N is the carrier density, J is the injection current density, e is the electronic charge, d is the active layer thickness of the laser, γ_{s} is the spontaneous carrier decay rate, n is the refractive index of the semiconductor medium, α is the coupling strength of the transmitter output to the receiver, and θ is the optical phase difference [14].

Based on the synchronization concept proposed by Kocarev and Parlitz [26], the existence of the identical synchronization solution $A^{\mathrm{R}} = A^{\mathrm{T}}$ requires that the rate equations of the transmitter and receiver be identical. This necessary condition for achieving chaos synchronization requires that $\theta = 0$, $\Delta\omega_{\mathrm{c}} = 0$ and the two lasers be identical except that $\gamma_{\mathrm{c}}^{\mathrm{R}} = \gamma_{\mathrm{c}}^{\mathrm{T}} + 2\eta\alpha$ [14]. From the steady-state condition of a free-running semiconductor laser, we further obtain the required detuning between the free-running frequencies of the transmitter and receiver due to the difference in γ_{c} as the following:

$$\omega_0^{\mathrm{T}} - \omega_0^{\mathrm{R}} = \Delta\omega_{\mathrm{c}} + (b^{\mathrm{T}}\gamma_{\mathrm{c}}^{\mathrm{T}} - b^{\mathrm{R}}\gamma_{\mathrm{c}}^{\mathrm{R}})/2.$$

When $\Delta\omega_{\mathrm{c}} = 0$, we obtain $\omega_0^{\mathrm{T}} - \omega_0^{\mathrm{R}} = (b^{\mathrm{T}}\gamma_{\mathrm{c}}^{\mathrm{T}} - b^{\mathrm{R}}\gamma_{\mathrm{c}}^{\mathrm{R}})/2$. Since $A^{\mathrm{T}}(t)$ and $A^{\mathrm{R}}(t)$ are both complex field amplitudes at the free-running frequency of the transmitter, complete chaos synchronization with $A^{\mathrm{R}} = A^{\mathrm{T}}$ requires that the optical frequency of the receiver be locked to that of the transmitter. It also requires that the fast-varying optical phase, the slow-varying phase, and the field amplitude of the receiver output all be synchronized to those of the transmitter output as well.

The identity between the rate equations of the transmitter and receiver is only the necessary condition for the system to achieve identical complete chaos synchronization. The sufficient condition to achieve chaos synchronization for this configuration was verified through a numerical simulation [14]. Based on the simulation result, the system can perform complete chaos synchronization when the coupling strength is beyond some value. For the effect of the mismatch on the laser internal parameters, the simulation result shows that the chaos synchronization of this system is very sensitive to γ_{c} and γ_{s}, but has large tolerance of the mismatch of b and other laser intrinsic parameters. In the experiment, we carefully choose two semiconductor lasers with different γ_{c}, but with very similar γ_{s} because of the objective of achieving parameter matching [14]. The coupling strength α can then be determined by the difference between $\gamma_{\mathrm{c}}^{\mathrm{T}}$ and $\gamma_{\mathrm{c}}^{\mathrm{R}}$ as $\alpha = \gamma_{\mathrm{c}}^{\mathrm{R}} - \gamma_{\mathrm{c}}^{\mathrm{R}}/2\eta$. The synchronization quality is measured through the correlation coefficient, denoted by ρ [7].

IV. ANALYSIS AND DISCUSSION

In the experiment, the threshold current of the transmitter is $I_{\mathrm{th}}^{\mathrm{T}} \simeq 21$ mA and the transmitter is biased above threshold at $I^{\mathrm{T}} = 2.38 I_{\mathrm{th}}^{\mathrm{T}}$. The injection strength from the master laser to the transmitter is adjusted so that the transmitter is operated in a chaotic state, of which the power spectrum is shown in Fig. 2(a) and the intensity wave form is shown in Fig. 2(b).

Generally, the most direct method to verify a chaotic state is to calculate the largest Lyapunov exponent, which characterizes the maximum trace divergence of the chaotic attractor. If it is positive, then the wave form is chaotic when there is no noise. However, measurement of the Lyapunov exponents is achievable only when, first, the real-time sampling resolution of the instrument for recording the time series is adequate and, second, the trace divergence from noise can be ignored in comparison with the trace divergence from the chaos characterized by positive Lyapunov exponents. Based on our analysis on the chaotic wave form generated from numerical simulation of the same system [14], the sampling rate of the instrument we used for recording the wave form is not sufficient to calculate the Lyapunov exponent for this high-speed complex dynamics. Instead, we use other characteristics—namely, the route to chaos, the nonperiodic wave form, and the broadband power spectrum—of chaos to verify it. As is shown in Fig. 2, the characteristics of the nonperiodic wave form and the broadband spectrum indicate that the transmitter is operated in a chaotic state. Under this operating condition, the frequency detuning of the MLD from the transmitter in free-running condition is 2.73 GHz. Since the numerical simulation at examining the characteristics of the chaos synchronization of the system has been performed at the choice of a chaotic state in the chaos region following the period-doubling route to chaos, we chose a chaotic state in the same chaos region to experimentally verify the result of the simulation and numerical analysis from our previous work [14].

The experimentally measured map of the nonlinear dynamics of the optically injected transmitter is shown in Fig. 3, in which the chaotic regions have been emphasized by

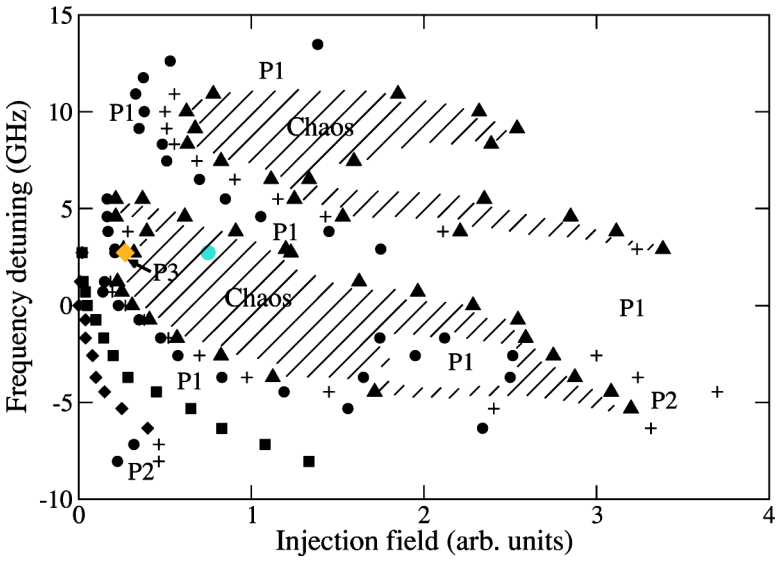

FIG. 3. Map of dynamical states of the transmitter laser subject to optical injection: Solid triangles indicate the boundary of the chaos regions; chaotic regions are emphasized by lines; solid circles indicate the boundary of period 1, P1; plus symbol marks the region of period 2, P2; solid squares mark the Hopf-bifurcation boundary; black solid diamonds indicate the saddle-node points; grey solid diamond indicates period-3 region, P3; grey solid circle indicates the operating point of the transmitter subject to the optical injection.

solid lines. The period-1 regions are marked or bounded by the solid circles, the period-2 regions are indicated by the plus symbols, the Hopf-bifurcation boundary is indicated by the solid squares, and the saddle-node line is indicated by the solid diamonds. The periodic regions outside the saddle-node boundary and a small period-3 region, marked by a grey solid diamond, which are reported in theoretical analysis and experiments [24], are also shown in Fig. 3. It is known that an optically injected semiconductor laser can perform different types of chaos [21]. The types of chaos are classified based on different routes to chaos. From the map, it shows that the chaotic state is reached through a period-doubling mechanism. A comparison between this experimental measured dynamical map to the other group's study [21,24] also verifies that the transmitter is operated in the chaotic region that follows the period-doubling route into chaos.

After careful adjustment of α and the injection strength from the MLD to the receiver, the receiver is synchronized to the transmitter when θ is zero. Under this operation condition, the optical power from the transmitter to the receiver is more than 10 times of that from the MLD to the receiver. Although the theory requires that the receiver be biased at $I^{\mathrm{R}}=2.38I_{\mathrm{th}}^{\mathrm{T}}$ to match I^{T}, the operation at $I^{\mathrm{R}}=I^{\mathrm{T}}$ does not lead to good synchronization. Instead, we found that biasing the receiver at $I^{\mathrm{R}}=1.95I_{\mathrm{th}}^{\mathrm{T}}=2.05I_{\mathrm{th}}^{\mathrm{R}}$, $I_{\mathrm{th}}^{\mathrm{R}}\simeq 20$ mA results in the best synchronization quality. Under this choice of receiver bias, the output powers of the transmitter and receiver match each other at a value of 4.02 mW. Indeed, the power of the transmitter output injecting into the receiver is definitely smaller than that of the transmitter output right at the transmitter's output facet because of optical components, shown in Fig. 1, between the transmitter and receiver. However, from the theory of chaos synchronization, when two chaotic lasers perform identical chaos synchronization, their output powers right in front of their respected output facets should be the same, and it is independent of the coupling strength once synchronization is achieved. This is also an important piece of evidence of the experimental observation as the true identical chaos synchronization. However, the bias currents for both lasers are usually not the same due to the parasitic effect of the laser diode packaging. Nevertheless, this implies that chaos synchronization in this system prefers the matching of the output optical power rather than the matching of the bias current if the matching on both cannot be satisfied simultaneously. It is also found that some power-dependent parameters of these two lasers are better matched when they are operated at the same output power than when they are biased at the same current level. The power spectrum of the synchronized receiver is shown in Fig. 4(a), which is very similar to that of the transmitter. The power spectrum of the

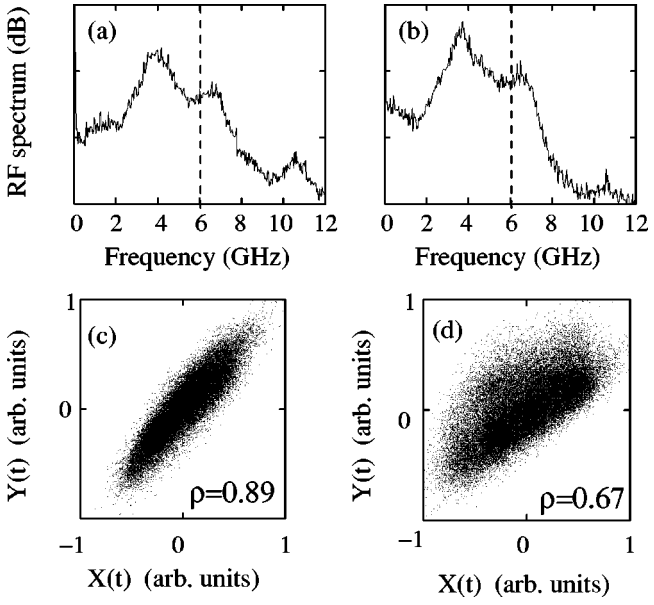

FIG. 4. Experimental result of chaos synchronization when $\theta=0$: (a) and (b) are power spectra of the receiver output and channel signal respectively; (c) correlation plot between the receiver output $X(t)$ and the transmitter output $Y(t)$; (d) correlation plot between the receiver output $X(t)$ and the channel signal $Y(t)$. Dashed lines in (a) and (b) indicate the 3-dB bandwidth, 6 GHz, of the photodiodes used for obtaining the power spectra. In reality, each power spectrum beyond 6 GHz is higher than the data shown here.

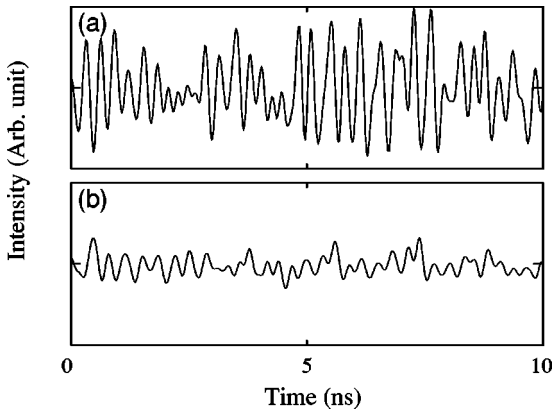

FIG. 5. Optical interference of synchronized fields from the transmitter and receiver: (a) constructive coherent interference, (b) destructive coherent interference.

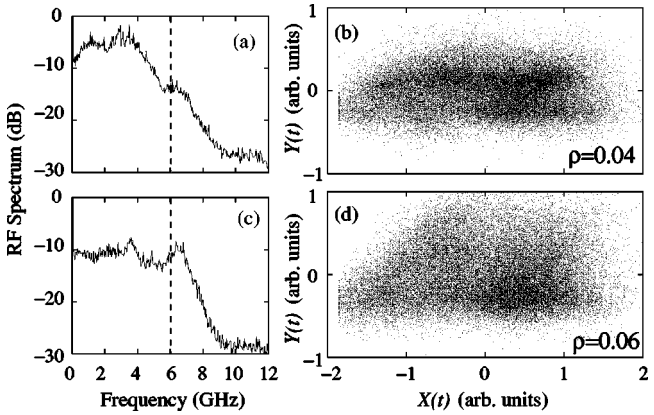

FIG. 6. Experimental result of chaos synchronization when $\theta=\pi$: (a) power spectrum of receiver output; (b) correlation plot between the receiver output $X(t)$ and the transmitter output $Y(t)$; (c) power spectrum of channel signal; (d) correlation plot between the receiver output $X(t)$ and the channel signal $Y(t)$. Dashed lines in (a) and (c) indicate the 3-dB bandwidth, 6 GHz, of the photodiodes used for obtaining the power spectra. In reality, each power spectrum beyond 6 GHz is higher than the data shown here.

channel signal as the superposition of the transmitter output and the MLD output is shown in Fig. 4(b).

The quality of the achieved synchronization with $\theta=0$ is demonstrated through the synchronization of the amplitude, the slow-varying phase, and the fast-varying optical phase. The synchronization of the chaotic amplitude is shown in Fig. 4(c) through the correlation plot between the intensities of the transmitter and receiver wave forms. The synchronization quality is measured to be $\rho\simeq 0.89$. The correlation between the channel signal and receiver wave forms is also measured and is found to be $\rho\simeq 0.67$ as shown in Fig. 4(d). Comparing the correlation plots in Figs. 4(c) and 4(d), we observed that the receiver is synchronized to the transmitter output, but not to the channel signal. This is a very important characteristic of identical chaos synchronization when the transmitter output is different from the signal coupled to the receiver.

The synchronization of the slow-varying chaotic phase and that of the fast-varying optical phase can be verified through the optical interference between the transmitter output and the receiver output by measuring the average ratio of the constructive interference to the destructive interference:

$$\text{ratio}=\frac{\overline{|A^{\mathrm{T}}|^2}+\overline{|A^{\mathrm{R}}|^2}+\overline{2|A^{\mathrm{T}}||A^{\mathrm{R}}|\cos(\phi^{\mathrm{T}}-\phi^{\mathrm{R}})}}{\overline{|A^{\mathrm{T}}|^2}+\overline{|A^{\mathrm{R}}|^2}-\overline{2|A^{\mathrm{T}}||A^{\mathrm{R}}|\cos(\phi^{\mathrm{T}}-\phi^{\mathrm{R}})}},$$

where $A^{\mathrm{T}}=|A^{\mathrm{T}}|e^{i\phi^{\mathrm{T}}}$ and $A^{\mathrm{R}}=|A^{\mathrm{R}}|e^{i\phi^{\mathrm{R}}}$. If $|A^{\mathrm{T}}|$ and $|A^{\mathrm{R}}|$ are completely uncorrelated, the term $\overline{2|A^{\mathrm{T}}||A^{\mathrm{R}}|\cos(\phi^{\mathrm{T}}-\phi^{\mathrm{R}})}$ will be zero. From the experiment, we knew that the intensity of the transmitter output is identically synchronized to that of the receiver output. Assuming that $|A^{\mathrm{R}}|=|A^{\mathrm{T}}|+\Delta A$, we have

$$\begin{aligned}\overline{2|A^{\mathrm{T}}||A^{\mathrm{R}}|\cos(\phi^{\mathrm{T}}-\phi^{\mathrm{R}})}&=\overline{2|A^{\mathrm{T}}|(|A^{\mathrm{T}}|+\Delta A)\cos(\phi^{\mathrm{T}}-\phi^{\mathrm{R}})}\\&=\overline{2|A^{\mathrm{T}}||A^{\mathrm{T}}|\cos(\phi^{\mathrm{T}}-\phi^{\mathrm{R}})}\\&\quad+\overline{2|A^{\mathrm{T}}|\Delta A\cos(\phi^{\mathrm{T}}-\phi^{\mathrm{R}})}\\&\simeq\overline{2|A^{\mathrm{T}}|^2\cos(\phi^{\mathrm{T}}-\phi^{\mathrm{R}})},\end{aligned}$$

since $|A^{\mathrm{T}}|$ and ΔA are uncorrelated, and ΔA is very small compared to $|A^{\mathrm{T}}|$. From the experiment, we have $\overline{|A^{\mathrm{T}}|^2}=\overline{|A^{\mathrm{R}}|^2}$. Therefore, we have the ratio as

$$\text{ratio}\simeq\frac{1+\overline{\cos(\phi^{\mathrm{T}}-\phi^{\mathrm{R}})}}{1-\overline{\cos(\phi^{\mathrm{T}}-\phi^{\mathrm{R}})}}.$$

. If their slow-varying phase and fast-varying phase are uncorrelated, the phase term $\overline{\cos(\phi^{\mathrm{T}}-\phi^{\mathrm{R}})}$ is zero. The value of the ratio is then about 1. From the experiment, we observed the optical interference with the result shown in Fig. 5. The intensity of the constructive coherent interference is shown in Fig. 5(a) and that of the destructive interference is shown in Fig. 5(b). The intensity extinction ratio is larger than 5. This provides evidence of synchronization of both the fast-varying and slow-varying phases as well as of the amplitude. As is expected from the theory, the entire optical field of the receiver is synchronized to that of the transmitter when identical chaos synchronization is achieved, and the receiver is synchronized to the transmitter rather than the channel signal, which is injected into the receiver.

Since the phase sensitivity is a very important characteristic of chaos synchronization in this system, the effect of phase mismatch has to be examined. As is anticipated by the theory, when we gradually tune θ away from zero without changing other operating conditions, the receiver quickly desynchronizes from the transmitter completely. The power spectrum of the desynchronized receiver is shown in Fig. 6(a). The correlation plot between the transmitter and receiver is shown in Fig. 6(b) and $\rho\simeq 0.04$. As a comparison, the power spectrum of the channel signal is shown in Fig. 6(c) and the synchronization quality between the receiver and channel signal is $\rho\simeq 0.06$. From the power spectra and the correlation plots shown in Fig. 4, we find that the receiver is not only desynchronized to the transmitter but has a higher output power than the transmitter output power when θ is improperly adjusted. The tolerance of this relative optical phase difference is around $\pm\pi/4$. The synchronization quality as a function of θ is shown in Fig. 7. The system has more tolerance of positive θ than of negative θ. This experi-

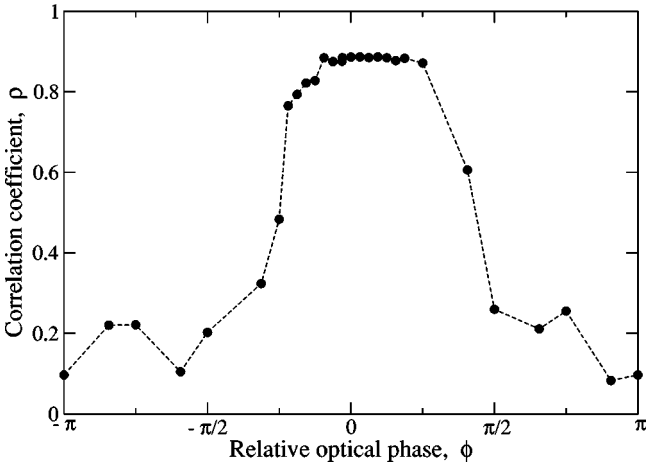

FIG. 7. Experimental result of synchronization quality as a function of the relative optical phase difference θ.

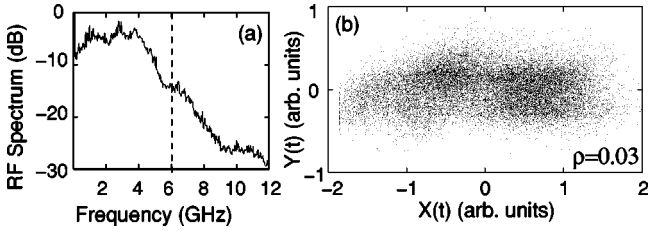

FIG. 8. Experimental result of chaos synchronization when MLD output to receiver is absent: (a) power spectrum of receiver output and (b) correlation plot between the receiver output $X(t)$ and the transmitter output $Y(t)$. Dashed line in (a) indicates the 3-dB bandwidth, 6 GHz, of the photodiode used for obtaining the power spectrum. In reality, the power spectrum beyond 6 GHz is higher than the data shown here.

mental result agrees with the theoretical analysis of this system [27]. The asymmetry of the phase sensitivity on the negative θ and the positive θ is due to the linewidth enhancement factor. From these observations, we can see that the complete synchronization in this system is sensitive to the optical phase θ with the sensitivity within a quarter of the wavelength.

Besides the phase sensitivity, the detuning between the free-running frequencies of the transmitter and receiver also serves as a characteristic of the chaos synchronization in this system. When synchronization is achieved, the free-running frequency of the receiver is detuned to that of the transmitter by about -32.6 ± 0.9 GHz. From the theory, we know that the required frequency detuning is $\omega_0^{\mathrm{T}}-\omega_0^{\mathrm{R}}=(b^{\mathrm{T}}\gamma_c^{\mathrm{T}}-b^{\mathrm{R}}\gamma_c^{\mathrm{R}})/2$ when the cold-cavity frequencies of both lasers are the same. From the measurement of laser parameters [25], we have $b^{\mathrm{T}}\simeq 12\simeq b^{\mathrm{R}}$ and $\gamma_c^{\mathrm{T}}-\gamma_c^{\mathrm{R}}\simeq -0.35\times 10^{11}\ \mathrm{s}^{-1}$. Because of this large linewidth factor, the positive locking boundary can reach beyond 12 GHz [28]. The upper locking boundary is determined by the product of $\sqrt{1+b^2}$ and A_{i} [29], the ratio of the strength of injection field to that of the intracavity field. Based on these measured laser parameters, the theoretical value of the detuning frequency between the free-running transmitter and the free-running receiver to achieve chaos synchronization is around -33.4 GHz. This value is in good agreement with the experimental observation. If we examine which state the receiver is locked to by setting the transmitter in the free-running condition, we find that the receiver is locked to the free-running transmitter in a bistable lock-unlock state [30]. Because of this frequency detuning between the transmitter and receiver, the frequency detuning between the MLD and receiver is around -29.87 GHz. Due to this large frequency detuning and the weak injection from the MLD to the receiver, the MLD alone cannot lock the receiver, but works more like an optical probe [25].

This observation suggests that the optical injection from the MLD to the receiver may not be necessary for achieving synchronization, whereas the injection of the MLD output to the receiver is important to retain the identical match between the configurations of the transmitter and receiver. It is then important to check if the receiver can still be synchronized to the transmitter when the optical injection from the MLD to the receiver is absent. The power spectrum of the receiver output under this operation condition is shown in Fig. 8(a), which is very different from the power spectrum of the transmitter output. The correlation plot between the transmitter and receiver is shown in Fig. 8(b) with $\rho\simeq 0.03$. As the result shows, the receiver cannot be synchronized to the transmitter without receiving the optical injection from the MLD though this injected optical field along cannot lock the optical frequency of the receiver. Therefore, receiving the weak optical injection from the MLD is crucial for the receiver to be synchronized to the transmitter. This demonstrates the need for matching the optical injection in making chaos synchronization in this system possible.

V. CONCLUSION

In conclusion, we have experimentally verified that frequency locking, phase synchronization, and amplitude synchronization for the high-frequency broadband chaotic optical fields of the transmitter and receiver are achieved in a fully optical system, where its chaotic optical wave form is generated through the high-speed nonlinearity of semiconductor lasers subject to optical injection. This experimentally achieved chaotic synchronous scenario is verified as identical chaos synchronization by observing several key characteristics of chaos synchronization in this system: The achieved synchronization is sensitive to the relative optical phase between the transmitter output and the master laser output when they are injected into the receiver. The experimental observation shows that the system can have a high synchronization quality when this phase is matched but is completely desynchronized when this phase is off by less than $\pi/2$. The experimental observed value of the detuning between the free-running frequencies of the transmitter and receiver also agrees very well with the theoretical value. Since the MLD output has to inject to both the transmitter and receiver to keep the configurations of these two lasers identical, the experimental result shows that a mismatch in the MLD output into these two lasers can completely destroy the achieved synchronization. The phase sensitivity, the frequency detuning condition, and the match requirement on the MLD output are the most significant characteristics to verify the observed

synchronous phenomenon as the identical chaos synchronization described by the chaos synchronization theory. It is also observed that the synchronization requires the close match in the laser parameters by operating the transmitter and receiver lasers at the same output power level if their bias currents might be different due to parasitic effects. The observation at the frequency detuning, the phase sensitivity, the effect of mismatch at the injection strength from the master laser, and match at the laser output power is in good agreement with the theoretical analysis of this system.

One important characteristic of this system is that the frequency detuning between the free-running transmitter and the free-running receiver is not zero, but is offset by the amount determined by the difference on the parameter γ_c, which is necessary for the system to achieve identical chaos synchronization. This characteristic is different from that of the optical feedback system studied by Liu *et al*. when complete chaos synchronization is achieved, in which the frequency detuning almost has to be strictly limited to zero [7]. With this limitation, the optical frequency of the receiver is always locked to that of the transmitter subject to optical feedback. However, since the frequency detuning in the optical injection system discussed in this paper can be offset more than 30 GHz, it would be interesting to numerically examine if the receiver can still be synchronized to the chaotic transmitter when this necessary frequency detuning results in the unlock of the receiver to the transmitter. As is indicated in this paper, the receiver is actually operated at the bistable region under the injection of the free-running transmitter. A question arises: Is the locking at the optical frequency a necessary condition for a fully optical system to achieve chaos synchronization or other chaotic synchronous scenarios? Besides this, it is possible that different types of chaos will have different characteristics even though they occur in the same system. It will be interesting to examine this topic.

ACKNOWLEDGMENTS

This work is supported by the U.S. Army Research Office under Contract No. DAAG55-98-1-0269.

[1] *Applications of Chaos in Modern Communication Systems* [IEEE Trans. Circuits Syst., I: Fundam. Theory Appl. 48, 1 (2001)].
[2] *Optical Chaos and Application to Cryptography* [IEEE J. Quantum Electron.38, 1 (2002)].
[3] C. Schafer, M. G. Rosenblum, J. Kurths, and H. Abbel, Nature (London) **392**, 239 (1998).
[4] R. Toral, C. Masoller, C. R. Mirasso, M. Ciszak, and O. Calvo, Physica A **325**, 192 (2003).
[5] I. Z. Kiss and J. L. Hudson, Phys. Rev. E **64**, 046215 (2001).
[6] M. Ciszak, O. Calvo, C. Masoller, C. R. Mirasso, and R. Toral, Phys. Rev. Lett. **90**, 204102 (2003).
[7] J. M. Liu, H. F. Chen, and S. Tang, IEEE J. Quantum Electron. **38**, 1184 (2002).
[8] Junji Ohtsubo, IEEE J. Quantum Electron. **38**, 1141 (2002).
[9] V. Kovanis, A. Gavrielides, T. B. Simpson, and J. M. Liu, Appl. Phys. Lett. **67**, 2780 (1995).
[10] M. W. Pan, B. P. Shi, and G. R. Gray, Opt. Lett. **22**, 166 (1997).
[11] J. Mork, B. Tromborg, and P. L. Christiansen, IEEE J. Quantum Electron. **24**, 123 (1998).
[12] S. Tang and J. M. Liu, IEEE J. Quantum Electron. **37**, 329 (2001).
[13] Y. Liu, Y. Takiguchi, P. Davis, T. Aida, S. Saito, and J. M. Liu, Appl. Phys. Lett. **80**, 4306 (2002).
[14] H. F. Chen and J. M. Liu, IEEE J. Quantum Electron. **36**, 27 (2000).
[15] S. Tang and J. M. Liu, Opt. Lett. **26**, 596 (2001).
[16] A. Locquet, C. Masoller, and C. R. Mirasso, Phys. Rev. E **65**, 056205 (2002).
[17] Raul Vicente, Toni Perez, and C. R. Mirasso, IEEE J. Quantum Electron. **38**, 1197 (2002).
[18] H. U. Voss, Phys. Rev. E **61**, 5115 (2000).
[19] T. Heil, I. Fischer, and W. Elsasser, Phys. Rev. Lett. **86**, 795 (2001).
[20] F. Y. Lin and J. M. Liu, IEEE J. Quantum Electron. **40**, 682 (2004).
[21] B. Krauskopf, S. Wieczorek, and D. Lenstra, Appl. Phys. Lett. **77**, 1611 (2000).
[22] S. Wieczorek, B. Krauskopf, and D. Lenstra, Opt. Commun. **183**, 215 (2000).
[23] T. B. Simpson and J. Liu, Opt. Commun. **112**, 43 (1994).
[24] S. Wieczorek, T. B. Simpson, B. Krauskopf, and D. Lenstra, Opt. Commun. **215**, 125 (2003).
[25] J. M. Liu and T. B. Simpson, IEEE J. Quantum Electron. **30**, 957 (1994).
[26] L. Kocarev and U. Parlitz, Phys. Rev. Lett. **74**, 5028 (1995).
[27] *Using Chaos for Digital Communication*, edited by L. E. Larson, J. M. Liu, and L. S. Tsimring, INLS series (Springer, New York, 2004), Chap. 9.
[28] H. F. Chen and J. M. Liu, IEEE J. Sel. Top. Quantum Electron. **10**, 918 (2004).
[29] T. B. Simpson, J. M. Liu, and A. Gavrielides, IEEE J. Quantum Electron. **32**, 1456 (1996).
[30] J. M. Liu, H. F. Chen, X. J. Meng, and T. B. Simpson, IEEE Photonics Technol. Lett. **9**, 1325 (1997).